Replicated transfer matrix analysis of Ising spin models on 'small world' lattices

T Nikoletopoulos†, A C C Coolen†, I Pérez Castillo‡, N S Skantzos§, J P L Hatchett† and B Wemmenhove¶

† Department of Mathematics, King's College London, The Strand, London WC2R 2LS, United Kingdom

‡ Institute for Theoretical Physics, Celestijnenlaan 200D, Katholieke Universiteit Leuven, B-3001 Belgium

§ Departament de Fisica Fonamental, Facultat de Fisica, Universitat de Barcelona, 08028 Barcelona, Spain

¶ Institute for Theoretical Physics, University of Amsterdam, Valckenierstraat 65, 1018 XE Amsterdam, The Netherlands

Abstract. We calculate equilibrium solutions for Ising spin models on 'small world' lattices, which are constructed by super-imposing random and sparse Poissonian graphs with finite average connectivity c onto a one-dimensional ring. The nearest neighbour bonds along the ring are ferromagnetic, whereas those corresponding to the Poisonnian graph are allowed to be random. Our models thus generally contain quenched connectivity and bond disorder. Within the replica formalism, calculating the disorder-averaged free energy requires the diagonalization of replicated transfer matrices. In addition to developing the general replica symmetric theory, we derive phase diagrams and calculate effective field distributions for two specific cases: that of uniform sparse long-range bonds (i.e. 'small world' magnets), and that of $\pm J$ random sparse long-range bonds (i.e. 'small world' spin-glasses).

1. Introduction

The concept of 'small world' networks [1] was introduced as an attempt to capture and study nontrivial features observed in realistic biological, technological and social networks. The key idea is to generate a structure which interpolates between a regular finite dimensional one and a sparse random long-range one. In a typical construction one starts with a locally regular network, e.g. a ring, where each site is connected to its $2k$ nearest neighbours, and subsequently 're-wires' randomly with a probability p those local connections, creating long range shortcuts. One characteristic of networks of this type, the so called 'small world effect', is that even for small p the average minimal
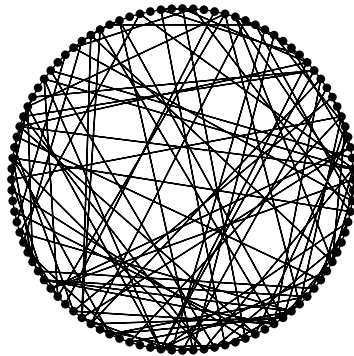
Figure 1. Example of a 'small world' lattice connecting N spins (indicated by $\bullet$) in the sense of our present models. Nearest neighbour interactions along a one-dimensional ring are combined with sparse long-range interactions in the form of a random Poissonian graph, with small average connectivity c. Here $N = 100$ and $c = 2$.

path length between two sites can still be very small. Small world networks have also attracted a lot of attention in physics [2, 3, 4, 5, 6]. A study of an Ising model [3] on a small world network showed that even for very small re-wiring probability p there exists a ferromagnetic phase transition at finite temperature, which is absent in the purely one-dimensional model. From a statistical mechanics point of view, the 'small world effect' can thus be thought of as inducing global order in a low-dimensional system by adding a small number of long range connections.

In this paper we study a family of Ising spin models defined on a lattice which, although not identical to the construction of [1], shares with the latter the 'small world' characteristics of a regular short-range structure in coexistence with a sparse and random range-free one. Our lattice consists of a one-dimensional ring of N sites occupied by Ising spins, where each site is firstly connected to its nearest neighbours, and secondly via a random Poissonian graph in which the average number of connections per site c remains finite in the thermodynamic limit $N \to \infty$. See e.g. figure 1. This architecture was also studied in [4]; however, the author of [4] did not attempt to calculate transition lines or phase diagrams analytically, but resorted to an annealed approximation. We take the bonds between nearest neighbours on the ring to be ferromagnetic, whereas the long-range bonds can be random. Our motivation for studying this structure is twofold. Firstly, our model is a combination of a one-dimensional system and a random finitely connected graph so its mathematical analysis is nontrivial yet feasible, requiring an interesting mixture of mathematical tools developed for one-dimensional models (the transfer matrix technique) and those developed for finite connectivity models. Finite connectivity techniques have been applied to many areas, such as error correcting codes [7, 8, 9], theoretical computer science [10, 11, 12, 13], neural networks [14, 15], and spin glasses [16, 17, 18, 20, 21, 22, 23]. In the later field, research has been triggered by the desire to develop solvable spin-glass models which are closer to real finite-dimensional

systems than the fully connected spin-glass model of [25]. The RKKY interactions of metallic spin-glasses can be regarded as a combination of short-range ferromagnetic bonds and long-range random ones. Thus there is a case for regarding our 'small world' networks, which are defined with a similar structure of spin-interactions, as perhaps more realistic than finite connectivity spin-glass models. This is our second motivation.

At a technical level, upon calculating for the present class of models an expression for the disorder-averaged free energy per spin using the replica formalism, one is led to a replicated transfer matrix structure embedded within a mean-field finite-connectivity type calculation. Solving our models thereby boils down to the diagonalization of specific $2^n \times 2^n$ replicated transfer matrices, in the limit $n \to 0$. We show how this can be done within the replica symmetric ansatz, and we use the result to calculate fully explicit expressions for transition lines, phase diagrams, and effective field distributions. Numerical simulations show perfect agreement with our theory.

Upon completion of this study, a preprint was communicated [27] in which the authors also aim to solve an Ising model on a small world lattice explicitly. However, both their methods (combinatorics rather than replicated transfer matrices) and model definitions (regular rather than random long-range sparse connectivity) differ from those in the present paper.

2. Definitions and replica analysis

Our model is a system of N interacting Ising spins $\sigma_i \in \{-1, 1\}$, in thermal equilibrium at inverse temperature $\beta = 1/T$, described by the following Hamiltonian (defined with $\sigma_{N+1} \equiv \sigma_1$):

$$H = -J_0 \sum_i \sigma_i \sigma_{i+1} - \frac{1}{c} \sum_{i<j} J_{ij} c_{ij} \sigma_i \sigma_j \tag{1}$$

The (long-range) couplings $J_{ij} \in \mathbb{R}$ are independent identically distributed random variables, drawn from some distribution $p(J_{ij})$. We will abbreviate $\int dJ \, p(J) g(J) = \langle g(J) \rangle_J$. The variables $c_{ij} \in \{0, 1\}$ specify whether a long-range bond between sites i and j is present ($c_{ij} = 1$) or absent ($c_{ij} = 0$); they are also independent random variables, drawn according to

$$p(c_{ij}) = \frac{c}{N} \delta_{c_{ij},1} + \left(1 - \frac{c}{N}\right) \delta_{c_{ij},0} \tag{2}$$

This choice leads in the thermodynamic limit $N \to \infty$ to a number of long range connections per site distributed according to a Poisson law with mean c. The number c will remain finite in the thermodynamic limit $N \to \infty$. Equilibrium ensemble averages, with the conventional Boltzmann measure for spin configurations, will simply be denoted by $\langle \ldots \rangle$. The dilution variables and long-range bonds $\{c_{ij}, J_{ij}\}$ represent quenched disorder, with respect to which all macroscopic thermodynamic quantities are assumed

to be self averaging in the limit $N \to \infty$. We will write disorder averages as $\overline{[\ldots]}$.

We calculate the asymptotic disorder-averaged free energy per spin in the conventional manner using the replica formalism, which is based on the identity

$$\overline{f} = -\lim_{N \to \infty} \frac{1}{\beta N} \lim_{n \to 0} \frac{1}{n} \log \overline{Z^n} \qquad Z = \sum_{\sigma_1,\ldots,\sigma_N} e^{-\beta H} \tag{3}$$

As usual, the disorder average is performed for integer n, the order of the limits $N \to \infty$ and $n \to 0$ is reversed, and the final result is extended to non-integer n to allow the limit $n \to 0$ to be taken. We will denote n-replicated spins by $\boldsymbol{\sigma}_i = (\sigma_1^i, \ldots, \sigma_n^i)$, and abbreviate $\{\boldsymbol{\sigma}\} = \{\boldsymbol{\sigma}_1, \ldots, \boldsymbol{\sigma}_N\}$. Averaging Z^n over the disorder now gives

$$\overline{Z^n} = \sum_{\{\boldsymbol{\sigma}\}} e^{\beta J_0 \sum_i \boldsymbol{\sigma}_i \cdot \boldsymbol{\sigma}_{i+1}} \overline{\left[e^{\frac{\beta}{c} \sum_{i<j} J_{ij} c_{ij} \boldsymbol{\sigma}_i \cdot \boldsymbol{\sigma}_j} \right]}$$

$$= \sum_{\{\boldsymbol{\sigma}\}} e^{\beta J_0 \sum_i \boldsymbol{\sigma}_i \cdot \boldsymbol{\sigma}_{i+1} + \frac{c}{N} \sum_{i<j} \langle e^{\frac{\beta J}{c} \boldsymbol{\sigma}_i \cdot \boldsymbol{\sigma}_j} - 1 \rangle_J + \mathcal{O}(N^0)} \tag{4}$$

This expression can be transformed into an integral to be calculated by steepest descent as $N \to \infty$, via the introduction of the order parameter distribution $P(\boldsymbol{s}; \{\boldsymbol{\sigma}\}) = N^{-1} \sum_i \delta_{\boldsymbol{s}, \boldsymbol{\sigma}_i}$. This latter observable gives the fraction of sites with a given configuration $\boldsymbol{s} \in \{-1, 1\}^n$ of replicated spin variables [21]. In particular we find

$$\overline{Z^n} = \int \prod_{\boldsymbol{s}} \left[\mathrm{d}P(\boldsymbol{s}) \mathrm{d}\hat{P}(\boldsymbol{s}) \right] e^{N\Psi[\{P, \hat{P}\}]} \tag{5}$$

$$\Psi[\{P, \hat{P}\}] = \mathrm{i} \sum_{\boldsymbol{s}} P(\boldsymbol{s}) \hat{P}(\boldsymbol{s}) + \frac{1}{2} c \sum_{\boldsymbol{s}, \boldsymbol{s}'} P(\boldsymbol{s}) P(\boldsymbol{s}') \langle e^{\frac{\beta J}{c} \boldsymbol{s} \cdot \boldsymbol{s}'} - 1 \rangle_J$$

$$+ \frac{1}{N} \log \sum_{\{\boldsymbol{\sigma}\}} e^{\beta J_0 \sum_i \boldsymbol{\sigma}_i \cdot \boldsymbol{\sigma}_{i+1} - \mathrm{i} \sum_i \hat{P}(\boldsymbol{\sigma}_i)} + \mathcal{O}(\frac{\log N}{N}) \tag{6}$$

In the limit $N \to \infty$ the integral (5) is dominated by the stationary point of $\Psi[\{P, \hat{P}\}]$. Working out the equations $\partial \Psi / \partial P(\boldsymbol{s}) = \partial \Psi / \partial \hat{P}(\boldsymbol{s}) = 0$, for all $\boldsymbol{s}$, gives respectively

$$\hat{P}(\boldsymbol{s}) = \mathrm{i} c \sum_{\boldsymbol{s}'} P(\boldsymbol{s}') \langle e^{\frac{\beta J}{c} \boldsymbol{s} \cdot \boldsymbol{s}'} - 1 \rangle_J \tag{7}$$

$$P(\boldsymbol{s}) = \lim_{N \to \infty} \frac{\sum_{\{\boldsymbol{\sigma}\}} e^{\beta J_0 \sum_i \boldsymbol{\sigma}_i \cdot \boldsymbol{\sigma}_{i+1} - \mathrm{i} \sum_i \hat{P}(\boldsymbol{\sigma}_i)} \left(\frac{1}{N} \sum_j \delta_{\boldsymbol{s}, \boldsymbol{\sigma}_j} \right)}{\sum_{\{\boldsymbol{\sigma}\}} e^{\beta J_0 \sum_i \boldsymbol{\sigma}_i \cdot \boldsymbol{\sigma}_{i+1} - \mathrm{i} \sum_i \hat{P}(\boldsymbol{\sigma}_i)}} \tag{8}$$

We use (7) to eliminate the conjugate order parameters. To proceed further we define a $2^n \times 2^n$ transfer matrix $\boldsymbol{T}[P]$ and a diagonal $2^n \times 2^n$ matrix $\boldsymbol{Q}[\boldsymbol{s}]$, with entries

$$T_{\boldsymbol{\sigma}, \boldsymbol{\sigma}'}[P] = e^{\beta J_0 \boldsymbol{\sigma} \cdot \boldsymbol{\sigma}' + c \sum_{\boldsymbol{s}} P(\boldsymbol{s}) \langle e^{\frac{\beta J}{c} \boldsymbol{\sigma} \cdot \boldsymbol{s}} - 1 \rangle_J} \tag{9}$$

$$Q_{\boldsymbol{\sigma}, \boldsymbol{\sigma}'}[\boldsymbol{s}] = \delta_{\boldsymbol{s}, \boldsymbol{\sigma}} \delta_{\boldsymbol{\sigma}, \boldsymbol{\sigma}'} \tag{10}$$

These definitions allow us to write the replicated spin summations as traces of matrix products, so that, upon inserting (7) into (8), the latter becomes

$$P(\boldsymbol{s}) = \lim_{N \to \infty} \frac{1}{N} \sum_j \frac{\mathrm{tr}(\boldsymbol{T}^{j-1}[P] \, \boldsymbol{Q}[\boldsymbol{s}] \, \boldsymbol{T}^{N-j+1}[P])}{\mathrm{tr}(\boldsymbol{T}^N[P])} = \lim_{N \to \infty} \frac{\mathrm{tr}(\boldsymbol{Q}[\boldsymbol{s}] \boldsymbol{T}^N[P])}{\mathrm{tr}(\boldsymbol{T}^N[P])} \tag{11}$$

Only contributions from the largest eigenvalue $\lambda(n; P)$ of (9) survive the limit $N \to \infty$. If we denote by $\boldsymbol{v}[P]$ and $\boldsymbol{u}[P]$ the associated left and right eigenvectors, with components $v_{\boldsymbol{\sigma}}[P]$ and $u_{\boldsymbol{\sigma}}[P]$, we arrive at the following expressions for (11) and the free energy:

$$P(\boldsymbol{s}) = \frac{v_{\boldsymbol{s}}[P] \ u_{\boldsymbol{s}}[P]}{\sum_{\boldsymbol{s}'} v_{\boldsymbol{s}'}[P] \ u_{\boldsymbol{s}'}[P]} \tag{12}$$

$$\overline{f} = \lim_{n \to 0} \frac{1}{n\beta} \left\{ \frac{1}{2} c \sum_{\boldsymbol{s}, \boldsymbol{s}'} P(\boldsymbol{s}) P(\boldsymbol{s}') \langle e^{\frac{\beta J}{c} \boldsymbol{s} \cdot \boldsymbol{s}'} - 1 \rangle_J - \log \lambda(n; P) \right\} \tag{13}$$

In order to proceed we next need to solve the eigenvalue problem for the replicated transfer matrix $\boldsymbol{T}[P]$ as defined in (9). This is generally a nontrivial task, therefore in the remainder of our paper we will focus on the replica symmetric solution.

3. Solution by diagonalization of RS replicated transfer matrix

3.1. Conversion to a functional eigenvalue problem

The ergodic, or replica symmetric (RS), ansatz corresponds to the distribution $P(\boldsymbol{s})$ being invariant under all permutations of the replica labels $\{1, \ldots, n\}$. Now $P(\boldsymbol{s})$ can depend on $\boldsymbol{s}$ only via the sum $\sum_{\alpha=1}^{n} s_\alpha$, and may thus always be written in the form

$$P(\boldsymbol{s}) = \int \mathrm{d}h \ W(h) \prod_{\alpha=1}^{n} \frac{e^{\beta h s_\alpha}}{2\cosh(\beta h)} \tag{14}$$

where the new RS order parameter $W(h)$ is a (normalized) distribution of effective fields h_i, which are defined via $\langle \sigma_i \rangle = \tanh(\beta h_i)$. Let us next define the following short-hand:

$$w(\sum_\alpha \sigma_\alpha, n) = \sum_{\boldsymbol{s}'} P(\boldsymbol{s}') \langle e^{\frac{\beta J}{c} \boldsymbol{\sigma} \cdot \boldsymbol{s}'} \rangle_J = \int \mathrm{d}h \ W(h) \frac{\langle e^{\beta[A(\frac{J}{c}, h)\sum_\alpha \sigma_\alpha + nB(\frac{J}{c}, h)]} \rangle_J}{[2\cosh(\beta h)]^n} \tag{15}$$

where

$$A(J, z) = \frac{1}{2\beta} \log \left[\frac{\cosh[\beta(J+z)]}{\cosh[\beta(J-z)]} \right] = \frac{1}{\beta} \operatorname{arctanh}[\tanh(\beta J)\tanh[\beta z]]$$

$$B(J, z) = \frac{1}{2\beta} \log \left[4\cosh[\beta(J+z)]\cosh[\beta(J-z)] \right]$$

This allows us to write the entries of our transfer matrix (9) within the RS ansatz as

$$T_{\boldsymbol{\sigma}, \boldsymbol{\sigma}'}^{\mathrm{RS}} = e^{\beta J_0 \boldsymbol{\sigma} \cdot \boldsymbol{\sigma}' + cw(\sum_\alpha \sigma_\alpha, n) - c}$$
$$= \int \mathrm{d}\hat{m} \ R(\hat{m}, n) \prod_\alpha e^{\beta J_0 \sigma_\alpha \sigma_\alpha' - i\beta \hat{m} \sigma_\alpha} \tag{16}$$

with

$$R(\hat{m}, n) = \beta \int \frac{\mathrm{d}m}{2\pi} \ e^{i\beta \hat{m} m + cw(m, n) - c} \tag{17}$$

The matrix (16) is formally identical to the replicated transfer matrix which would have been found for Ising chains with (complex) random fields $-i\hat{m}$, distributed according to $R(\hat{m}, n)$. We exploit this equivalence, and postulate eigenvectors with the structure as found in one-dimensional random-field models. In particular, for the right and left

eigenvectors of the largest eigenvalue of (16) we substitute a form which is a complex extension of that introduced in [26]:

$$u_{\boldsymbol{\sigma}}^{\mathrm{RS}} = \int \mathrm{d}x_1 \mathrm{d}x_2 \ \Phi(x_1, x_2|n) \ e^{\beta(x_1 + \mathrm{i}x_2) \sum_\alpha \sigma_\alpha} \tag{18}$$

$$v_{\boldsymbol{\sigma}}^{\mathrm{RS}} = \int \mathrm{d}y_1 \mathrm{d}y_2 \ \Psi(y_1, y_2|n) \ e^{\beta(y_1 + \mathrm{i}y_2) \sum_\alpha \sigma_\alpha} \tag{19}$$

In one-dimensional models $x_1 + \mathrm{i}x_2$ and $y_1 + \mathrm{i}y_2$ would represent fields which are propagated along the chain, according to a random Markovian map which reflects the statistical properties of the random fields and nearest neighbour interactions. In the limit $N \to \infty$, $\Phi(\dots|n)$ and $\Psi(\dots|n)$ give the distributions of these fields, invariant under the map. Insertion of (18,19) into the eigenvalue equations (to be satisfied for every $\boldsymbol{\sigma}$), i.e.

$$\sum_{\boldsymbol{\sigma}'} T_{\boldsymbol{\sigma}, \boldsymbol{\sigma}'}^{\mathrm{RS}} u_{\boldsymbol{\sigma}'}^{\mathrm{RS}} = \lambda_{\mathrm{RS}}(n) u_{\boldsymbol{\sigma}}^{\mathrm{RS}}, \qquad \sum_{\boldsymbol{\sigma}'} v_{\boldsymbol{\sigma}'}^{\mathrm{RS}} T_{\boldsymbol{\sigma}', \boldsymbol{\sigma}}^{\mathrm{RS}} = \lambda_{\mathrm{RS}}(n) v_{\boldsymbol{\sigma}}^{\mathrm{RS}}$$

leads to new eigenvalue problems for Φ and Ψ, with $\boldsymbol{x} = (x_1, x_2)$ and $\boldsymbol{y} = (y_1, y_2)$:

$$\lambda_{\mathrm{RS}}(n)\Phi(\boldsymbol{x}|n) = \int \mathrm{d}\boldsymbol{x}' \ \Lambda_\Phi(\boldsymbol{x}, \boldsymbol{x}'|n) \ \Phi(\boldsymbol{x}'|n) \tag{20}$$

$$\lambda_{\mathrm{RS}}(n)\Psi(\boldsymbol{y}|n) = \int \mathrm{d}\boldsymbol{y}' \ \Lambda_\Psi(\boldsymbol{y}, \boldsymbol{y}'|n) \ \Psi(\boldsymbol{y}'|n) \tag{21}$$

with the complex kernels

$$\Lambda_\Phi(\boldsymbol{x}, \boldsymbol{x}'|n) = \int \mathrm{d}\hat{m} \ R(\hat{m}, n) \ e^{n\beta B(J_0, x_1' + \mathrm{i}x_2')} \ \delta \begin{pmatrix} x_1 - \mathrm{Re}\{A(J_0, x_1' + \mathrm{i}x_2') - \mathrm{i}\hat{m}\} \\ x_2 - \mathrm{Im}\{A(J_0, x_1' + \mathrm{i}x_2') - \mathrm{i}\hat{m}\} \end{pmatrix} \tag{22}$$

$$\Lambda_\Psi(\boldsymbol{y}, \boldsymbol{y}'|n) = \int \mathrm{d}\hat{m} \ R(\hat{m}, n) \ e^{n\beta B(J_0, y_1' + \mathrm{i}y_2' - \mathrm{i}\hat{m})} \ \delta \begin{pmatrix} y_1 - \mathrm{Re} \ A(J_0, y_1' + \mathrm{i}y_2' - \mathrm{i}\hat{m}) \\ y_2 - \mathrm{Im} \ A(J_0, y_1' + \mathrm{i}y_2' - \mathrm{i}\hat{m}) \end{pmatrix} \tag{23}$$

In order to find a self-consistent equation for the RS order parameter $W(h)$ in (14) we need to inspect only the $n \to 0$ limit of the eigenvalue problems (20,21). For the free energy, however, we need to know the first two orders in n of the eigenvalue $\lambda_{\mathrm{RS}}(n)$.

3.2. Derivation of the RS order parameter equation

Upon taking the limit $n \to 0$ we find the kernels (22,23) reducing to

$$\Lambda_\Phi(\boldsymbol{x}, \boldsymbol{x}'|0) = \int \mathrm{d}\hat{m} \ R(\hat{m}, 0) \ \delta \begin{pmatrix} x_1 - \mathrm{Re}\{A(J_0, x_1' + \mathrm{i}x_2') - \mathrm{i}\hat{m}\} \\ x_2 - \mathrm{Im}\{A(J_0, x_1' + \mathrm{i}x_2') - \mathrm{i}\hat{m}\} \end{pmatrix} \tag{24}$$

$$\Lambda_\Psi(\boldsymbol{y}, \boldsymbol{y}'|0) = \int \mathrm{d}\hat{m} \ R(\hat{m}, 0) \ \delta \begin{pmatrix} y_1 - \mathrm{Re} \ A(J_0, y_1' + \mathrm{i}y_2' - \mathrm{i}\hat{m}) \\ y_2 - \mathrm{Im} \ A(J_0, y_1' + \mathrm{i}y_2' - \mathrm{i}\hat{m}) \end{pmatrix} \tag{25}$$

Subsequent integration of the eigenvalue equations (20,21) over $\boldsymbol{x}$ and $\boldsymbol{y}$, for $n \to 0$ and using $\int \mathrm{d}\boldsymbol{x} \ \Phi(\boldsymbol{x}|0) > 0$ and $\int \mathrm{d}\boldsymbol{y} \ \Psi(\boldsymbol{y}|0) > 0$ (since Φ and Ψ represent field distributions), leads in both cases to the following identity

$$\lambda_{\mathrm{RS}}(0) = \int \mathrm{d}\hat{m} \ R(\hat{m}, 0) = e^{cw(0,0)-c} = 1 \tag{26}$$

which is indeed necessary for the $n \to 0$ limit in (13) to exist. Knowing $\lambda_{\mathrm{RS}}(0)$, we may in turn write the two $n \to 0$ eigenvalue problems as

$$\Phi(\boldsymbol{x}|0) = \int \mathrm{d}\boldsymbol{x}' \; \Phi(\boldsymbol{x}'|0) \int \frac{\mathrm{d}z\mathrm{d}m}{2\pi} e^{\mathrm{i}zm+cw(m,0)-c} \; \delta \left(\begin{array}{c} x_1 - \mathrm{Re}\{A(J_0, x_1'+\mathrm{i}x_2') - \frac{\mathrm{i}z}{\beta}\} \\ x_2 - \mathrm{Im}\{A(J_0, x_1'+\mathrm{i}x_2') - \frac{\mathrm{i}z}{\beta}\} \end{array} \right)$$

$$\Psi(\boldsymbol{y}|0) = \int \mathrm{d}\boldsymbol{y}' \; \Psi(\boldsymbol{y}'|0) \int \frac{\mathrm{d}z\mathrm{d}m}{2\pi} e^{\mathrm{i}zm+cw(m,0)-c} \; \delta \left(\begin{array}{c} y_1 - \mathrm{Re}\; A(J_0, y_1'+\mathrm{i}y_2' - \frac{\mathrm{i}z}{\beta}) \\ y_2 - \mathrm{Im}\; A(J_0, y_1'+\mathrm{i}y_2' - \frac{\mathrm{i}z}{\beta}) \end{array} \right)$$

We now expand $e^{cw(m,0)}$ in powers of c, using $w(m,0) = \int \mathrm{d}h \; W(h)\langle e^{\beta m A(\frac{J}{c},h)}\rangle_J$:

$$\int \frac{\mathrm{d}z\mathrm{d}m}{2\pi} e^{\mathrm{i}zm+cw(m,0)-c}\delta\left(\ldots\right) = \sum_{k\geq 0} \frac{e^{-c}c^k}{k!} \int \frac{\mathrm{d}z\mathrm{d}m}{2\pi} \; e^{\mathrm{i}zm} w^k(m,0)\delta\left(\ldots\right)$$

$$= \sum_{k\geq 0} \frac{e^{-c}c^k}{k!} \int \prod_{\ell=1}^k [\mathrm{d}h_\ell \mathrm{d}J_\ell W(h_\ell)p(J_\ell)] \int \frac{\mathrm{d}z\mathrm{d}m}{2\pi} \delta\left(\ldots\right) e^{\mathrm{i}zm+\beta m \sum_{\ell=1}^k A(\frac{J_\ell}{c},h_\ell)}$$

We assume our functions to decay to zero sufficiently fast away from the origin to allow us to shift the z-integration in the complex plane according to $z \to z+\mathrm{i}\beta \sum_{\ell=1}^k A(\frac{J_\ell}{c},h_\ell)$. This enables us to perform the integral over m, giving $2\pi\delta(z)$, and write

$$\Phi(\boldsymbol{x}|0) = \int \mathrm{d}\boldsymbol{x}' \; \Phi(\boldsymbol{x}'|0) \sum_{k\geq 0} \frac{e^{-c}c^k}{k!} \int \prod_{\ell=1}^k [\mathrm{d}h_\ell \mathrm{d}J_\ell W(h_\ell)p(J_\ell)]$$

$$\times \delta \left(\begin{array}{c} x_1 - \mathrm{Re}\{A(J_0, x_1'+\mathrm{i}x_2') + \sum_{\ell=1}^k A(\frac{J_\ell}{c},h_\ell)\} \\ x_2 - \mathrm{Im}\{A(J_0, x_1'+\mathrm{i}x_2') + \sum_{\ell=1}^k A(\frac{J_\ell}{c},h_\ell)\} \end{array} \right) \tag{27}$$

$$\Psi(\boldsymbol{y}|0) = \int \mathrm{d}\boldsymbol{y}' \; \Psi(\boldsymbol{y}'|0) \sum_{k\geq 0} \frac{e^{-c}c^k}{k!} \int \prod_{\ell=1}^k [\mathrm{d}h_\ell \mathrm{d}J_\ell W(h_\ell)p(J_\ell)]$$

$$\times \delta \left(\begin{array}{c} y_1 - \mathrm{Re}\; A(J_0, y_1'+\mathrm{i}y_2' + \sum_{\ell=1}^k A(\frac{J_\ell}{c},h_\ell)) \\ y_2 - \mathrm{Im}\; A(J_0, y_1'+\mathrm{i}y_2' + \sum_{\ell=1}^k A(\frac{J_\ell}{c},h_\ell)) \end{array} \right) \tag{28}$$

These eigenvalue equations allow for solutions describing the expected manifestly real-valued fields, i.e. $\Phi(x_1, x_2|0) = \delta(x_2)\Phi(x_1)$ and $\Psi(y_1, y_2|0) = \delta(y_2)\Psi(y_1)$, where

$$\Phi(x) = \int \mathrm{d}x' \; \Phi(x') \sum_{k\geq 0} \frac{e^{-c}c^k}{k!} \int \prod_{\ell=1}^k [\mathrm{d}h_\ell \mathrm{d}J_\ell W(h_\ell)p(J_\ell)]$$

$$\times \delta[x - A(J_0, x') - \sum_{\ell=1}^k A(\frac{J_\ell}{c},h_\ell)] \tag{29}$$

$$\Psi(y) = \int \mathrm{d}y' \; \Psi(y') \sum_{k\geq 0} \frac{e^{-c}c^k}{k!} \int \prod_{\ell=1}^k [\mathrm{d}h_\ell \mathrm{d}J_\ell W(h_\ell)p(J_\ell)]$$

$$\times \delta[y - A(J_0, y' + \sum_{\ell=1}^k A(\frac{J_\ell}{c},h_\ell))] \tag{30}$$

We may always normalize our solutions such that $\int \mathrm{d}x \; \Phi(x) = \int \mathrm{d}y \; \Psi(y) = 1$, which will be assumed from now on. Finally, for RS states (14,18,19) with $\Phi(x_1, x_2|0) = \delta(x_2)\Phi(x_1)$ and $\Psi(y_1, y_2|0) = \delta(y_2)\Psi(y_1)$ we find the self-consistency equation (12) reducing to

$$\int \mathrm{d}h \; W(h) \frac{e^{\beta h \sum_\alpha s_\alpha}}{[2\cosh(\beta h)]^n} = \frac{\int \mathrm{d}x\mathrm{d}y \; \Phi(x)\Psi(y)e^{\beta(x+y)\sum_\alpha s_\alpha}}{\int \mathrm{d}x\mathrm{d}y \; \Phi(x)\Psi(y)[2\cosh[\beta(x+y)]]^n} \tag{31}$$

From this we obtain for $n = 0$ the simple expression

$$W(h) = \int dx dy \ \Phi(x)\Psi(y)\delta[h - x - y] \tag{32}$$

The final trio of coupled equations (29,30,32), to be solved simultaneously, determine the effective field distributions $W(h), \Phi(x), \Psi(y)$. The latter functions play the role of RS order parameters in our theory.

3.3. Derivation of the RS free energy

We now turn to the evaluation of the free energy per spin in RS ansatz, by inserting (14) into (13):

$$\overline{f}_{\mathrm{RS}} = \lim_{n \to 0} \frac{c}{2n\beta} \left\langle \int dh dh' \ W(h)W(h') \left[\frac{\sum_{\sigma,\sigma'} e^{\beta(h\sigma + h'\sigma' + \frac{J}{c}\sigma\sigma')}}{4\cosh(\beta h)\cosh(\beta h')} \right]^n - 1 \right\rangle_J$$

$$- \lim_{n \to 0} \frac{1}{n\beta} \log \lambda_{\mathrm{RS}}(n)$$

$$= \frac{c}{2\beta} \int dh dh' \ W(h)W(h')\langle \log[1 + \tanh(\frac{\beta J}{c})\tanh(\beta h)\tanh(\beta h')]\rangle_J$$

$$+ \frac{c}{2\beta}\langle \log\cosh(\frac{\beta J}{c})\rangle_J - \lim_{n \to 0} \frac{1}{n\beta} \log \lambda_{\mathrm{RS}}(n) \tag{33}$$

In evaluating $\lambda_{\mathrm{RS}}(n)$ we will need the following two identities:

$$w(0, n) \qquad = 1 + n\int dh \ W(h)\left\{\beta\langle B(\frac{J}{c}, h)\rangle_J - \log[2\cosh(\beta h)]\right\} + \mathcal{O}(n^2) \tag{34}$$

$$\int d\hat{m} \ R(\hat{m}, n) = e^{cw(0,n) - c}$$

$$= 1 + nc\int dh \ W(h)\left\{\beta\langle B(\frac{J}{c}, h)\rangle_J - \log[2\cosh(\beta h)]\right\} + \mathcal{O}(n^2) \tag{35}$$

We can now obtain an expression for $\lambda_{\mathrm{RS}}(n)$ by integrating both sides of equation (20):

$$\lim_{n \to 0} \frac{1}{n} \log \lambda_{\mathrm{RS}}(n) = \lim_{n \to 0} \frac{1}{n} \log \left\{ \frac{\int d\boldsymbol{x} d\boldsymbol{x}' \ \Lambda_\Phi(\boldsymbol{x}, \boldsymbol{x}'|n) \ \Phi(\boldsymbol{x}'|n)}{\int d\boldsymbol{x} \ \Phi(\boldsymbol{x}|n)} \right\}$$

$$= \lim_{n \to 0} \frac{1}{n} \log \left\{ \frac{\int d\boldsymbol{x} \ \int d\hat{m} \ R(\hat{m}, n) e^{n\beta B(J_0, x_1 + ix_2)} \ \Phi(\boldsymbol{x}|n)}{\int d\boldsymbol{x} \ \Phi(\boldsymbol{x}|n)} \right\}$$

$$= c\int dh \ W(h)\left\{\beta\langle B(\frac{J}{c}, h)\rangle_J - \log[2\cosh(\beta h)]\right\}$$

$$+ \beta \int dx \ \Phi(x)B(J_0, x) \tag{36}$$

Insertion into (33) subsequently gives, after some simple manipulations:

$$\overline{f}_{\mathrm{RS}} = \frac{c}{2\beta} \int dh dh' \ W(h)W(h')\langle \log[1 + \tanh(\frac{\beta J}{c})\tanh(\beta h)\tanh(\beta h')]\rangle_J$$

$$- \frac{c}{2\beta} \int dh \ W(h)\langle \log[1 - \tanh^2(\frac{\beta J}{c})\tanh^2(\beta h)]\rangle_J$$

$$- \frac{c}{2\beta}\langle \log\cosh(\frac{\beta J}{c})\rangle_J$$

$$- \frac{1}{2\beta} \int dx \ \Phi(x) \log\left[4\cosh[\beta(J_0 + x)]\cosh[\beta(J_0 - x)]\right] \tag{37}$$

4. General mathematical properties of our RS equations

4.1. Special limits

Let us first confirm that for the two extreme choices $p(J) = \delta(J)$ (equivalently $c = 0$, where we return to a simple ferromagnetic ring) and $J_0 = 0$ (where we retain only the sparse Poissonian graph) we recover from our present full RS theory the appropriate simpler equations known from earlier literature, to serve as benchmark tests.

We will repeatedly benefit from the property $A(0, z) = 0$. For $p(J) = \delta(J)$ our RS order parameter equations (29,30) simply give $\Phi(x) = \Psi(x)$ for all x, with

$$\Phi(x) = \int \mathrm{d}x' \ \Phi(x')\delta[x - A(J_0, x')] \tag{38}$$

Any solution Φ of this equation can have support only at periodic points of the non-linear map $x \to A(J_0, x)$. Upon writing $y = \tanh(\beta J_0)\tanh(\beta x)$ this map can be simplified to $y \to \tanh(\beta J_0)y$, so the only periodic point is the trivial fixed-point $x = 0$. It follows that the only normalized solution of (38) is $\Phi(x) = \delta(x)$, with which we obtain the trivial effective field distribution $W(h) = \delta(h)$, as we should, and the correct free energy of the one-dimensional Ising model:

$$\overline{f}_{\mathrm{RS}} = -\frac{1}{\beta}\log[2\cosh(\beta J_0)] \tag{39}$$

For $J_0 = 0$, on the other hand, our order parameter equations tell us that $\Psi(y) = \delta(y)$ and hence $W(h) = \Phi(h)$. Now we recover the familiar equation for $W(h)$ corresponding to purely Poissonian finite connectivity spin-glass models, which can be found in e.g. [18]:

$$W(h) = \sum_{k \geq 0} \frac{e^{-c}c^k}{k!} \int \prod_{\ell=1}^{k} [\mathrm{d}h_\ell \mathrm{d}J_\ell W(h_\ell)p(J_\ell)]$$
$$\times \delta\left[h - \frac{1}{\beta}\sum_{\ell=1}^{k} \mathrm{arctanh}[\tanh(\frac{\beta J_\ell}{c})\tanh(\beta h_\ell)]\right] \tag{40}$$

4.2. Scalar RS observables

The conventional RS scalar observables such as the magnetization m and the spin-glass order parameter q can be obtained as always as integrals over the effective field distribution $W(h)$. The starting point are the usual replica identities

$$\overline{\langle\sigma_i\rangle} = \lim_{n \to 0}\frac{1}{n}\sum_\alpha \sum_{\{\boldsymbol{\sigma}\}} \sigma_i^\alpha \overline{\left[\prod_{\gamma=1}^{n} e^{-\beta H(\boldsymbol{\sigma}^\gamma)}\right]}$$

$$\overline{\langle\sigma_i\rangle^2} = \lim_{n \to 0}\frac{1}{n(n-1)}\sum_{\alpha \neq \beta} \sum_{\{\boldsymbol{\sigma}\}} \sigma_i^\alpha \sigma_i^\beta \overline{\left[\prod_{\gamma=1}^{n} e^{-\beta H(\boldsymbol{\sigma}^\gamma)}\right]}$$

Upon repeating all those manipulations which we followed previously in calculating the RS free energy, one arrives at the familiar expressions for $m = \lim_{N \to \infty} N^{-1}\sum_i \overline{\langle\sigma_i\rangle}$ and

$q = \lim_{N\to\infty} N^{-1} \sum_i \overline{\langle\sigma_i\rangle^2}$:

$$m = \int dh \; W(h) \tanh(\beta h) \qquad q = \int dh \; W(h) \tanh^2(\beta h) \qquad (41)$$

4.3. Continuous bifurcations away from the paramagnetic state

Inspection of the three coupled equations (29,30,32) shows that, due to $A(J,0) = 0$, the paramagnetic state $\Phi(h) = \Psi(h) = W(h) = \delta(h)$ is always a solution. For $\beta = 0$ (high temperatures), where $A(J,z) = 0$ for any (J,z), it is the only solution. As always in finite connectivity theory, we can find continuous bifurcations away from the paramagnetic solution (upon lowering the temperature) by assuming that close to the transition the effective fields are very narrowly distributed around zero. This enables us to expand our equations in moments of the field distributions. We make the ansatz $\int dh \; h^k \Phi(h) = \mathcal{O}(\epsilon^k)$ and $\int dh \; h^k \Psi(h) = \mathcal{O}(\epsilon^k)$, with $|\epsilon| \ll 1$, so that also

$$m = \beta \int dx \; \Phi(x)x + \beta \int dy \; \Psi(y)y + \mathcal{O}(\epsilon^3) \qquad (42)$$

$$q = \beta^2 \int dxdy \; \Phi(x)\Psi(y)(x+y)^2 + \mathcal{O}(\epsilon^3) \qquad (43)$$

Bifurcations in which the lowest non-zero order is ϵ thus describe transitions towards a ferromagnetic state (P→F), and those where the lowest non-zero order is ϵ^2 transitions towards a spin-glass state (P→SG). The P→F transitions therefore follow upon expanding the first order moments of (29,30), putting $\overline{x} = \int dx \; x\Phi(x)$ and $\overline{y} = \int dy \; y\Psi(y)$ and using $A(J,z) = z \tanh(\beta J) + \mathcal{O}(z^3)$:

$$\overline{x} = \tanh(\beta J_0)\overline{x} + c\langle\tanh(\frac{\beta J}{c})\rangle_J(\overline{x} + \overline{y}) + \mathcal{O}(\epsilon^3) \qquad (44)$$

$$\overline{y} = \tanh(\beta J_0)\overline{y} + c\tanh(\beta J_0)\langle\tanh(\frac{\beta J}{c})\rangle_J(\overline{x} + \overline{y}) + \mathcal{O}(\epsilon^3) \qquad (45)$$

From this one deduces that a continuous $m \neq 0$ bifurcation occurs at

$$\text{P} \to \text{F}: \qquad 1 = c \langle\tanh(\frac{\beta J}{c})\rangle_J \; e^{2\beta J_0} \qquad (46)$$

Similarly we find the P→SG transitions upon expanding the second order moments of (29,30), assuming $\overline{x} = \overline{y} = 0$ and putting $\overline{x^2} = \int dx \; x^2\Phi(x)$ and $\overline{y^2} = \int dy \; y^2\Psi(y)$:

$$\overline{x^2} = \tanh^2(\beta J_0)\overline{x^2} + c\langle\tanh^2(\frac{\beta J}{c})\rangle_J(\overline{x^2} + \overline{y^2}) + \mathcal{O}(\epsilon^3) \qquad (47)$$

$$\overline{y^2} = \tanh^2(\beta J_0)\overline{y^2} + c\tanh^2(\beta J_0)\langle\tanh^2(\frac{\beta J}{c})\rangle_J(\overline{x^2} + \overline{y^2}) + \mathcal{O}(\epsilon^3) \qquad (48)$$

From this one deduces that a continuous bifurcation of $q > 0$ (while $m = 0$) occurs at

$$\text{P} \to \text{SG}: \qquad 1 = c \langle\tanh^2(\frac{\beta J}{c})\rangle_J \; \cosh(2\beta J_0) \qquad (49)$$

For $\beta = 0$ the right-hand sides of (46,49) are both zero, so the actual (second order) physical transition will occur at the highest temperature for which either of the two right-hand sides has increased to unity.

In the next two sections we will work out our theory for two particular simple choices for the Poissonian long-range bond distribution $p(J)$. Numerical evidence suggests that first order transitions away from the paramagnetic state are absent.

5. Small world systems with non-disordered bonds

We first choose $p(J_{ij}) = \delta[J_{ij} - J]$ with $J \geq 0$, i.e. uniform sparse long-range ferromagnetic bonds (for $J \leq 0$ there can obviously never be any transition).

5.1. The phase diagram

The second order transition lines (46) and (49) now reduce to

$$\mathrm{P} \to \mathrm{F}: \qquad 1 = c \ \tanh(\frac{\beta J}{c}) \ e^{2\beta J_0} \tag{50}$$

$$\mathrm{P} \to \mathrm{SG}: \qquad 1 = c \ \tanh^2(\frac{\beta J}{c}) \ \cosh(2\beta J_0) \tag{51}$$

Since $\cosh(2\beta J_0) \leq e^{2\beta J_0}$ and $\tanh^2(\beta J/c) \leq \tanh(\beta J/c)$ for $J \geq 0$, the P→SG instability cannot occur as it will always be preceded by the P→F one. As expected we find only the P and F phases. The equation from which to solve the transition temperature T_F can be rewritten as

$$\beta J = \frac{1}{2}c \ \log\left[\frac{c + e^{-2\beta J_0}}{c - e^{-2\beta J_0}}\right] \tag{52}$$

In the limit $c \to \infty$ we find condition (52) reducing to $\beta J = e^{-2\beta J_0}$. This expression has been found earlier in the context of $1 + \infty$ dimensional attractor neural networks [24].

We note in (52) that ferromagnetic order requires $\beta J_0 > \log(1/\sqrt{c})$; this inequality always holds when $c > 1$, and puts a finite upper bound on T_F when $c < 1$. Given $\beta J_0 > \log(1/\sqrt{c})$ and $J_0 > 0$, however, there will now always be a solution $T_\mathrm{F} > 0$. The simple equation (52) thus reveals the 'small world' effect in statistical mechanical terms: for any nonzero average Poissonian connectivity c (including $c < 1$) and all non-zero bond strengths $\{J_0, J\}$ (however small) there exists a *finite* transition temperature $T_\mathrm{F}(J_0, J, c)$ where ferromagnetism sets in. Since the pure Poissonian graph (i.e. $J_0 = 0$) would exhibit a transition only when $c > 1$, above the percolation threshold, this result is not obvious. One can apparently induce an overall non-zero magnetization in the one-dimensional ferromagnetic ring by adding a very small number of long range connections. Similarly, the one-dimensional ring leads to the emergence of a non zero magnetization even when superimposed on random graphs with $c < 1$, below the percolation threshold.

We have drawn the line (52) in a $(\beta J_0, \beta J)$ phase diagram, for different values of the average Poissonian connectivity c, in figure 2. Lowering the temperature from $T = \infty$ down to $T = 0$ corresponds in this diagram to moving along a straight line, with slope given by J/J_0, away from the origin $(\beta J_0, \beta J) = (0, 0)$.

5.2. Effective field distributions

To appreciate the physics in the ordered state of the small world magnet, we also solved numerically the order parameter equations (29,30,32), which here simplify to

$$\Phi(x) \;=\; \int \mathrm{d}x' \ \Phi(x') \sum_{k \geq 0} \frac{e^{-c}c^k}{k!} \int \prod_{\ell=1}^{k} [\mathrm{d}h_\ell W(h_\ell)] \ \delta[x - A(J_0, x') - \sum_{\ell=1}^{k} A(\frac{J}{c}, h_\ell)] \tag{53}$$
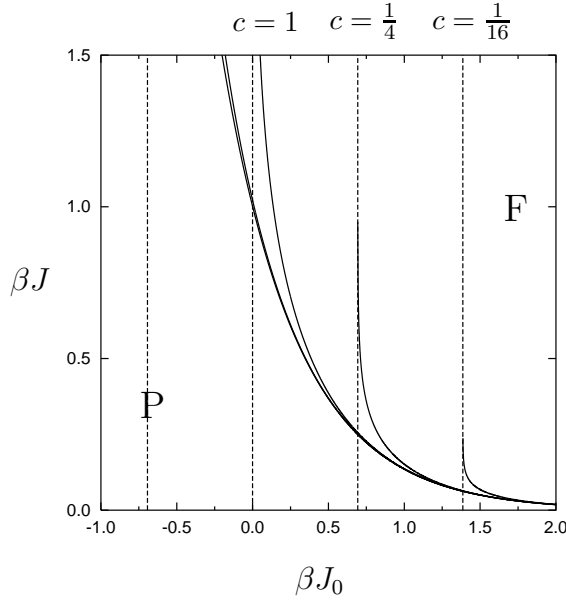
Figure 2. Phase diagram in the $(\beta J_0, \beta J)$ plane of the 'small world' magnet (i.e. uniform sparse long-range bonds), defined by $H = -J_0 \sum_i \sigma_i \sigma_{i+1} - \frac{J}{c} \sum_{i<j} c_{ij} \sigma_i \sigma_j$. Solid lines: P→F transition lines for $c = \frac{1}{16}, \frac{1}{4}, 1, 4, 16$ (from right to left). Dashed vertical lines: asymptotic values $\beta J_0 = \log(1/\sqrt{c})$ at which the critical values of βJ diverge (and below which no order is possible), for $c = \frac{1}{16}, \frac{1}{4}, 1, 4$ (from right to left). This diagram demonstrates the so called 'small world effect'. Along the axis $\beta J = 0$ we have a one-dimensional model, where there is no phase transition at finite temperature. Along the $\beta J_0 = 0$ axis we have the random finitely connected graph, where a P→F transition is known to exist at $\beta J = \frac{1}{2} c \log[(c+1)/(c-1)]$, provided $c > 1$ (i.e. above the percolation threshold). When the two structures are combined we always find a phase transition at finite temperature, for any value of c (however small).

$$\Psi(y) = \int dy' \ \Psi(y') \sum_{k \geq 0} \frac{e^{-c} c^k}{k!} \int \prod_{\ell=1}^{k} [dh_\ell W(h_\ell)] \ \delta[y - A(J_0, y' + \sum_{\ell=1}^{k} A(\frac{J}{c}, h_\ell))] \quad (54)$$

$$W(h) = \int dx dy \ \Phi(x) \Psi(y) \delta[h - x - y] \quad (55)$$

The results are shown in figure 3 for two choices of control parameters in the ferromagnetic region: for $T = 1$, $c = 10$, $J_0 = \frac{1}{4}$ and $J = 1$ (i.e. above the percolation threshold of the Possionian graph) and for $T = \frac{3}{2}$, $c = \frac{1}{2}$, $J_0 = 1$ and $J = \frac{3}{5}$ (i.e. below the percolation threshold). In the first case the effective field distributions are found to be smooth. For $c < 1$, however, the distributions are seen to be highly irregular.

5.3. Comparison with simulations

To complete our analysis for the small world magnet we have compared the predicted values for m and q of our solution as obtained by numerical solution of (53,54,55), followed by evaluation of (41), with the result of numerical simulation of the stochastic microscopic dynamics, taken to be of the conventional Glauber type and with $N = 10,000$. In the present (non-frustrated) small world magnet equilibration is found to
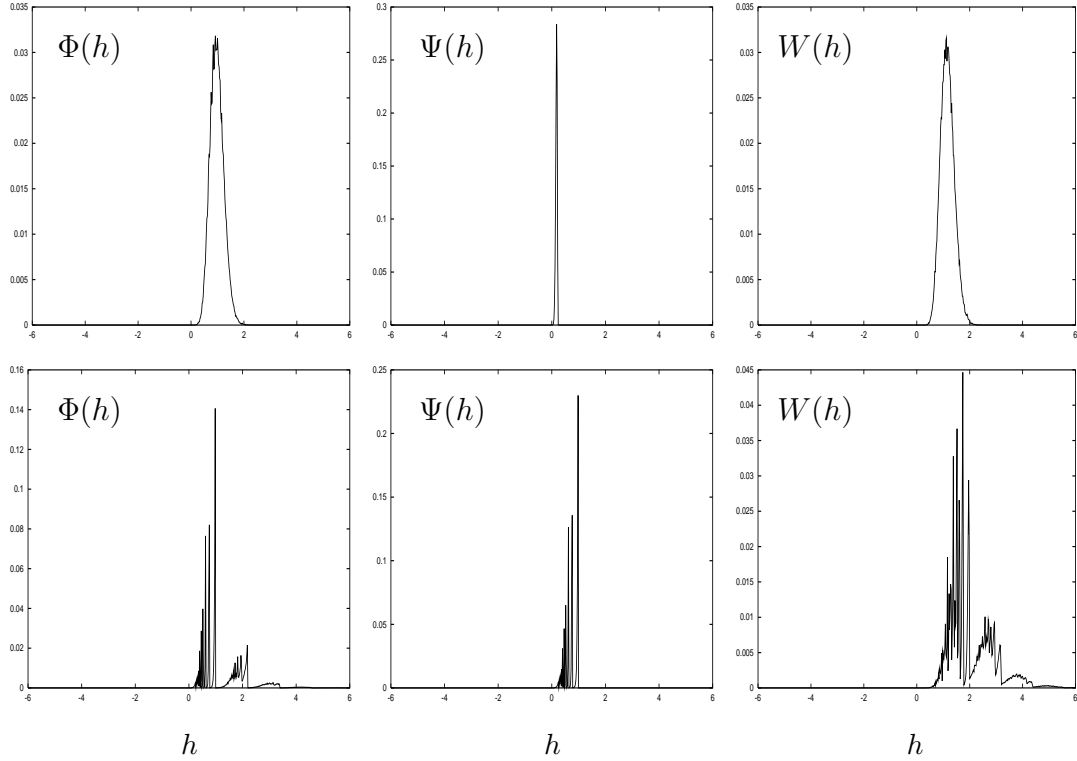
Figure 3. Effective field distributions for the 'small world' ferromagnet (i.e. uniform sparse long-range bonds), defined by $H = -J_0 \sum_i \sigma_i \sigma_{i+1} - \frac{J}{c} \sum_{i<j} c_{ij} \sigma_i \sigma_j$, as obtained by numerical solution of the order parameter equations (29,30,32) in the ferromagnetic phase. Top row: distributions well above the percolation threshold of the Poissonian graph ($T = 1$, $c = 10$, $J_0 = \frac{1}{4}$ and $J = 1$). Bottom row: distributions for a system below the percolation threshold and for more dominant chain bonds ($T = \frac{3}{2}$, $c = \frac{1}{2}$, $J_0 = 1$ and $J = \frac{3}{5}$). Note that the vertical scales used in the two rows are not identical.

be relatively easy to achieve, as a result of which the agreement between theory and experiment is found to be very good. Examples are shown in figure 4, for parameter values identical to those used earlier to produce the field distributions in figure 3.

6. Small world spin glasses

We finally work out our theoretical predictions for a 'small world' spin-glass, where the sparse long range bonds are truly random, and distributed according to $p(J_{ij}) = p\delta(J_{ij} - J) + (1 - p)\delta(J_{ij} + J)$. Without loss of generality we may take $J \geq 0$.

6.1. The phase diagram

The second order transition lines (46) and (49) now take the form

$$\text{P} \to \text{F}: \qquad 1 = c(2p - 1)\tanh(\frac{\beta J}{c})\, e^{2\beta J_0} \tag{56}$$

$$\text{P} \to \text{SG}: \qquad 1 = c\,\tanh^2(\frac{\beta J}{c})\,\cosh(2\beta J_0) \tag{57}$$
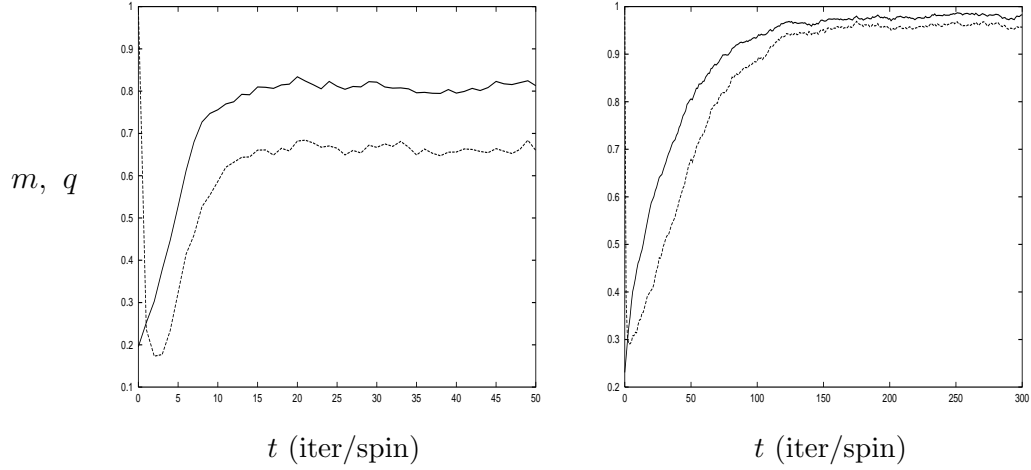
Figure 4. Observables m (solid lines) and q (dashed lines) as measured during numerical simulations of the 'small world' magnet, for $N = 10,000$. Left: $T = 1$, $c = 10$, $J_0 = \frac{1}{4}$ and $J = 1$. Here the theory predicts the equilibrium values $m = 0.80$ and $q = 0.65$. Right: $T = \frac{2}{3}$, $c = \frac{1}{2}$, $J_0 = 1$ and $J = \frac{3}{5}$. Here the theory predicts the equilibrium values $m \simeq 0.98$ and $q \simeq 0.96$. In both cases equilibration is achieved relatively fast, and the agreement between theory and simulations is very good.
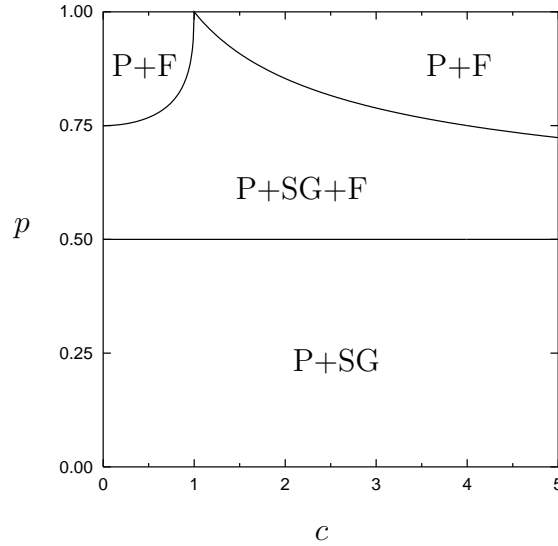
Figure 5. The possible phases of the 'small world' spin-glass for the different allowed combinations of the dimensionless control parameters $c \geq 0$ (the average Poissonian connectivity) and $p \in [0, 1]$ (the probability of $J_{ij} = +J$ in the Poissonian bonds).

Now both transitions may generally occur, dependent on the values of p and c, unless $p \leq \frac{1}{2}$ where only the P$\rightarrow$SG transition is possible. For $c \rightarrow \infty$ we see that only the P$\rightarrow$F transition will remain. We will transform the above equations into the dimensionless

variables $x = J_0/J$ and $y = T/J$, which gives for the P→F transition

$$\mathrm{P} \to \mathrm{F}: \qquad x_\mathrm{F} = \frac{1}{2}y \log\left[(2p-1)c\tanh(1/yc)\right]^{-1} \qquad (p \geq \frac{1}{2} \text{ only}) \quad (58)$$

$$y \to 0: \qquad x_\mathrm{F} = \frac{1}{2}y \log\left[(2p-1)c\right]^{-1} + \dots$$

$$y \to \infty: \qquad x_\mathrm{F} = \frac{1}{2}y \log\left[y/(2p-1)\right] + \dots$$

The line will intersect the $x = 0$ axis at $y = 1/c \log\sqrt{[(2p-1)c+1]/[(2p-1)c-1]}$, provided $c < 1/(2p-1)$. The P→SG transition line now takes the form

$$\mathrm{P} \to \mathrm{SG}: \qquad x_\mathrm{SG} = \frac{1}{2}y \log\left[\frac{1 + \sqrt{1 - c^2\tanh^4(1/yc)}}{c\tanh^2(1/yc)}\right] \qquad (59)$$

$$y \to 0: \qquad x_\mathrm{SG} = \frac{1}{2}y \log\left[(1 + \sqrt{1 - c^2})/c\right] + \dots \qquad (c \leq 1 \text{ only})$$

$$y \to \infty: \qquad x_\mathrm{SG} = \frac{1}{2}y \log\left[2cy^2\right] + \dots$$

Clearly, the physics for $c > 1$ will again be significantly different from that found for $c \leq 1$. If $c \leq 1$ one will have a P→SG transition for any $y > 0$, whereas for $c > 1$ it will only occur when $y > 2/c \log[(\sqrt{c} + 1)/(\sqrt{c} - 1)]$. The two transition lines can meet at a triple point, which is found to be the solution of

$$\text{triple point } (x^\star, y^\star): \qquad \begin{cases} \tanh(1/y^\star c) = (2p-1)\left[1 + \sqrt{1 - c^2\tanh^4(1/y^\star c)}\right] \\ x^\star = \frac{1}{2}y^\star \log\left[(2p-1)c\tanh(1/y^\star c)\right]^{-1} \end{cases} \quad (60)$$

Graphical inspection of the equation $\tau = (2p-1)[1 + \sqrt{1 - c^2\tau^4}]$ shows that the necessary and sufficient existence condition for the triple point are:

$$c \leq 1: \qquad 2p - 1 \leq \frac{1}{1 + \sqrt{1 - c^2}}, \qquad c \geq 1: \qquad 2p - 1 \leq \frac{1}{\sqrt{c}} \qquad (61)$$

We may conclude, since $\lim_{y\to\infty} x_\mathrm{F}/x_\mathrm{SG} = 0$, that as long as $p > \frac{1}{2}$ there will be a P→F transition, but that a P→SG transition exists if and only if (61) is satisfied (if not, the P→F transition will always happen first). Thus, the possible phases (dependent on the remaining energy-related control parameters T, J, J_0) are

$$p \leq \frac{1}{2}: \ \{\mathrm{P}, \mathrm{SG}\} \qquad \frac{1}{2} < p < p_c: \ \{\mathrm{P}, \mathrm{SG}, \mathrm{F}\} \qquad p \geq p_c: \ \{\mathrm{P}, \mathrm{F}\}$$

where

$$p_{c\leq 1} = \frac{1}{2} + \frac{1}{2(1 + \sqrt{1 - c^2})} \qquad p_{c\geq 1} = \frac{1}{2} + \frac{1}{2\sqrt{c}}$$

This is summarized in figure 5. We are not yet able to determine the F→SG transition (if both F and SG phases exist) analytically, since this would require us to solve our equations also below the P→F and/or P→SG transition temperatures. However we may put forward the conjecture (which seems reasonable on the basis of our experience with more conventional disordered spin models, e.g. [25, 28, 29]), that, especially upon taking RSB into account (if needed), there will be no change of phase type after the
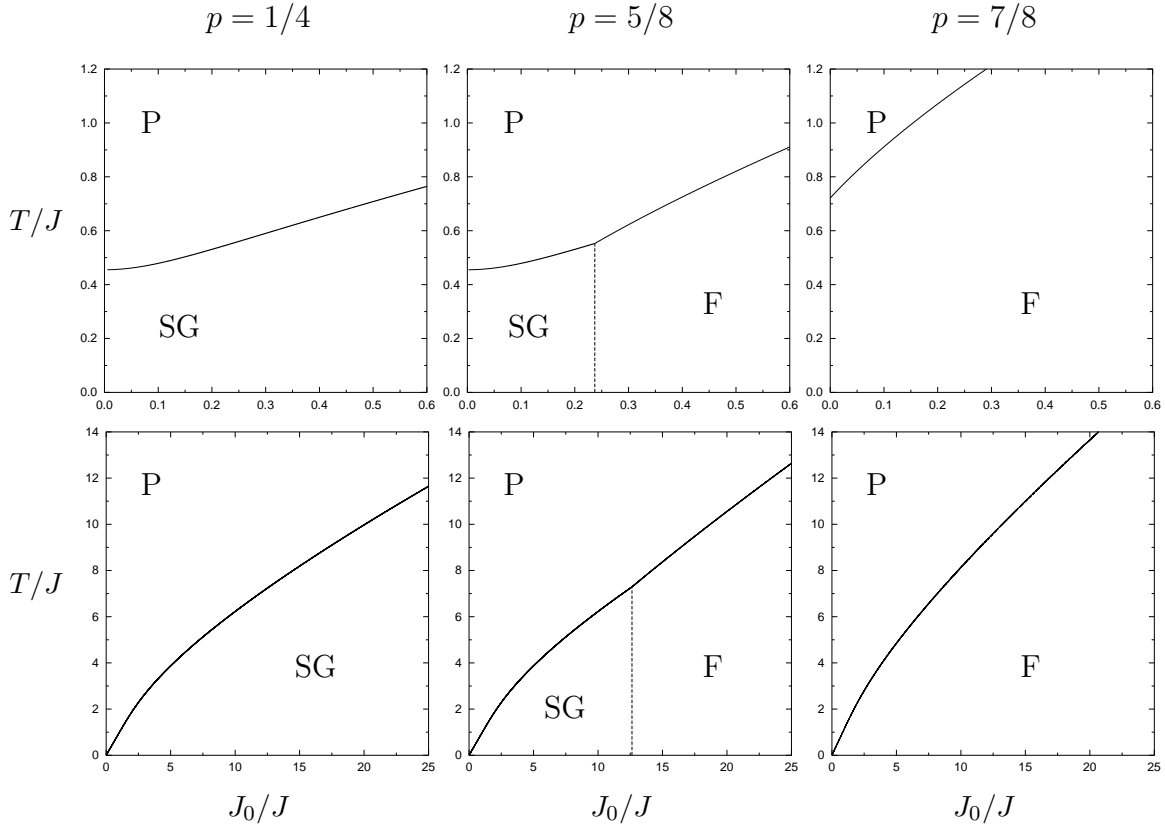
Figure 6. Phase diagrams in the $(J_0/J, T/J)$ plane for 'small world' spin glasses, i.e. ferromagnetic rings with random sparse long-range bonds with strengths distributed according to $p(J_{ij}) = p\delta[J_{ij} - J] + (1-p)\delta[J_{ij} + J]$. Here $p \in \{\frac{1}{4}, \frac{5}{8}, \frac{7}{8}\}$. The P→F and P→SG transitions (solid lines) and the triple point follow from our theory. The F→SG transition (dashed) is obtained upon using the location of the triple point in combination with the conjecture that on lowering temperature the nature of the ordered phase will remain that which emerges at the onset. Top row: $c = 4$, well above the percolation threshold of the Poissonian graph. Bottom row: $c = 1/4$, well below the percolation threshold. Here neither the ring nor the Poissonian graph would have exhibited order, whereas the combination does (the 'small world' effect).

onset of order as the temperature is lowered from $T = \infty$ to $T = 0$. This conjecture would predict the elusive F→SG transition to be the line segment in the (x, y) plane going from $(x^\star, 0)$ to $(x^\star, y^\star)$, where the latter is the triple point (60).

In figure 6 we show typical examples of the resulting phase diagrams in the $(J_0/J, T/J)$ plane, probing systematically the regimes exhibited in figure 5. It should be noted that, in spite of the equivalent notation and the resulting temptation to make hasty comparisons, the parameter J only has a meaning identical to that in the SK spin-glass [25], i.e. measuring the variance in the bonds, for $p = \frac{1}{2}$. The P→SG instability line is independent of p, in contrast to the P→F one. We observe here that, as the fraction p of positive long-range bonds increases (for fixed connectivity c) from $p < \frac{1}{2}$ (where there can be no ferromagnetic phase) to larger values, the ferromagnetic phase becomes
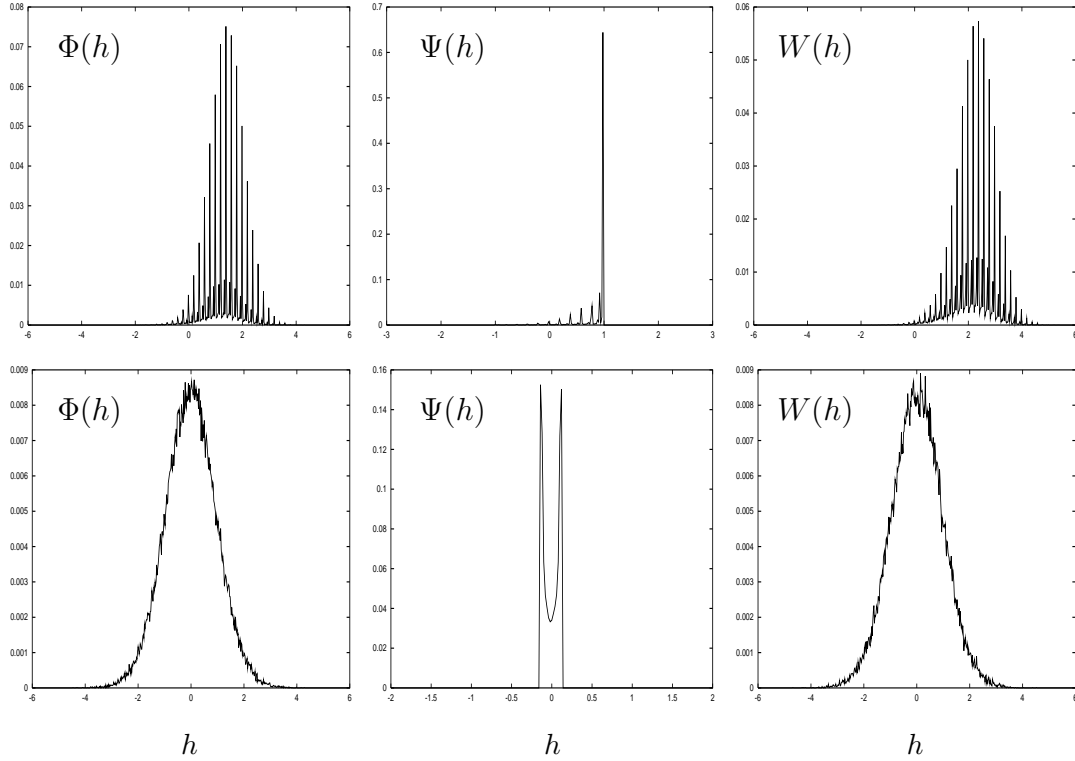
Figure 7. Effective field distributions for 'small world' spin glasses, i.e. ferromagnetic rings with random sparse long-range bonds with strengths distributed according to $p(J_{ij}) = p\delta[J_{ij} - J] + (1 - p)\delta[J_{ij} + J]$. Here we show examples for $c = 10$, i.e. well above the percolation threshold of the Poissonian graph, in the spin-glass phase, with $p = 5/8$. Top row: $J_0/J = 1/2$ and $T/J = 1/10$ (here the presence of the ring is important). Bottom row: $J_0/J = 1/32$ and $T/J = 1/8$ (here the physics is dominated by the sparse long-range bonds).

increasingly important, to the point where it destroys the spin-glass phase altogether. However, there is again a clear difference between $c > 1$, where even without the ring (i.e. for $J_0 = 0$) an ordered state is possible, and $c < 1$ (below the percolation threshold of the Poissonian graph) where as in the case of the small world magnet it is the 'small world' effect which generates global order.

6.2. Effective field distributions

Also for the small world spin-glass we have solved numerically the order parameter equations (29,30,32), resulting in figures 7, 8 and 9. It will be clear that, especially at low temperatures and around or below the percolation threshold, the effective field distributions can acquire highly nontrivial shapes (especially when compared to the Gaussian effective field distributions which one typically finds in non-diluted bond-disordered spin models). Furthermore, increasing the bond strength J_0 along the ring has the effect of changing field distributions from being smooth into more discretized shapes, similar to what is found in random field and random bond Ising chains [30, 31, 32].
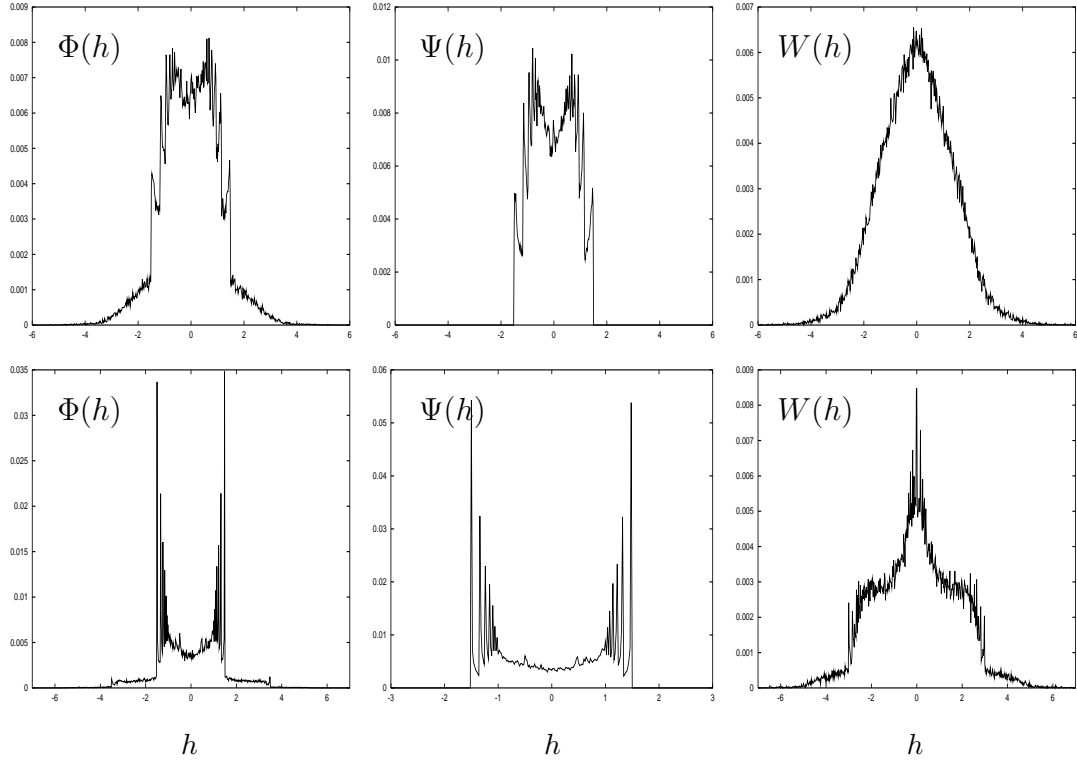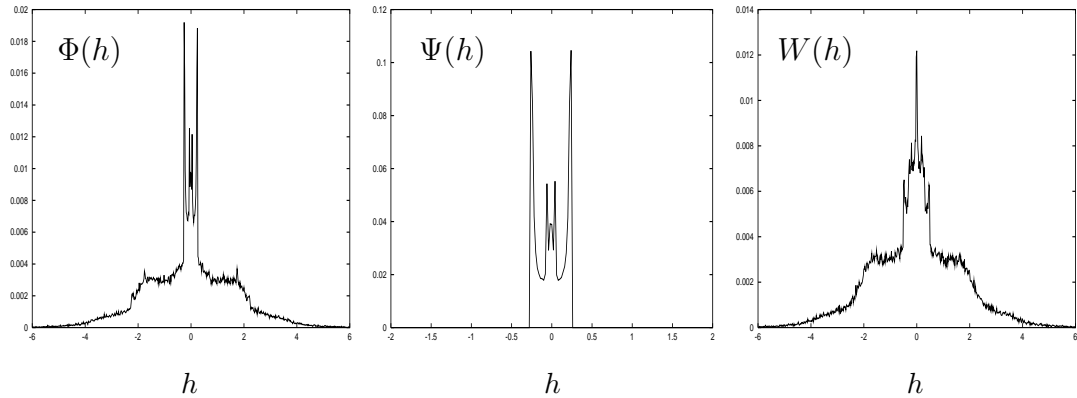
Figure 8. Effective field distributions for 'small world' spin glasses, i.e. ferromagnetic rings with random sparse long-range bonds with strengths distributed according to $p(J_{ij}) = p\delta[J_{ij} - J] + (1 - p)\delta[J_{ij} + J]$. Here we show examples for $c = \frac{1}{2}$, i.e. well below the percolation threshold of the Poissonian graph (where the 'small world' effect dominates), again in the spin-glass phase, with $p = 5/8$ and $J_0/J = 3/2$. Top row: $T/J = 1$. Bottom row: $T/J = 1/2$.

Figure 9. Effective field distributions for 'small world' spin glasses, i.e. ferromagnetic rings with random sparse long-range bonds with strengths distributed according to $p(J_{ij}) = p\delta[J_{ij} - J] + (1 - p)\delta[J_{ij} + J]$. Here we show examples for $c = 2$, i.e. just above the percolation threshold of the Poissonian graph, again in the spin-glass phase, with $p = 3/4$, $J_0/J = 1/16$ and $T/J = 1/4$.
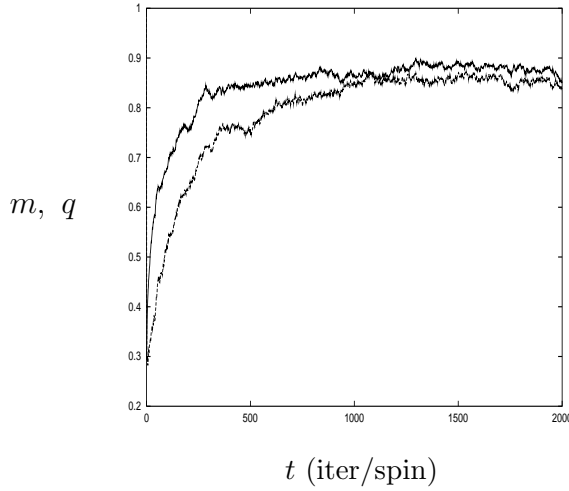
t (iter/spin)

Figure 10. Observables m (solid lines) and q (dashed lines) as measured during numerical simulations of the 'small world' spin-glass for $N = 10,000$. We show equilibration in the ferromagnetic phase, below the percolation threshold of the Poissonian graph ($p = 3/4$, $T = 1$, $c = 0.5$, $J_0 = 2$ and $J = 0.5$). Here the theory predicts the equilibrium values $m \simeq 0.84$ and $q \simeq 0.83$. Compared to the small world magnet, equilibration is harder to achieve, but the agreement between theory and simulations is still very good.

6.3. Comparison with simulations

We have finally compared the predicted values for m and q of our solution, as obtained by numerical solution of (29,30,32), followed by evaluation of (41), with the result of numerical simulation of the stochastic microscopic dynamics (of the conventional Glauber type) with $N = 10,000$. In contrast to the small world magnet, in the small world spin-glass equilibration is found to be not only much slower but also more subject to finite size fluctuations. However, the agreement between theory and experiment is still found to be very good. Examples are shown in figure 10.

7. Discussion

In this paper we have analyzed Ising spin models on 'small world' lattices, consisting of a combination of a one-dimensional ferromagnetic periodic chain and a sparse (finitely connected) random Poissonian graph with (generally) random bonds, using the replica method. Upon making a replica symmetric ansatz, we have been able to diagonalize the relevant replicated transfer matrices, and thereby obtain explicit expressions for the asymptotic free energy per spin and the continuous transitions away from the paramagnetic phase to either a ferromagnetic or a spin-glass one. We believe our results to constitute the first rigorous solution for this type of hybrid random 'small world' Ising spin model (given the RS ansatz), of relevance therefore both in the context of 'small world' models as such, but also in terms of the methodology used (diagonalization of
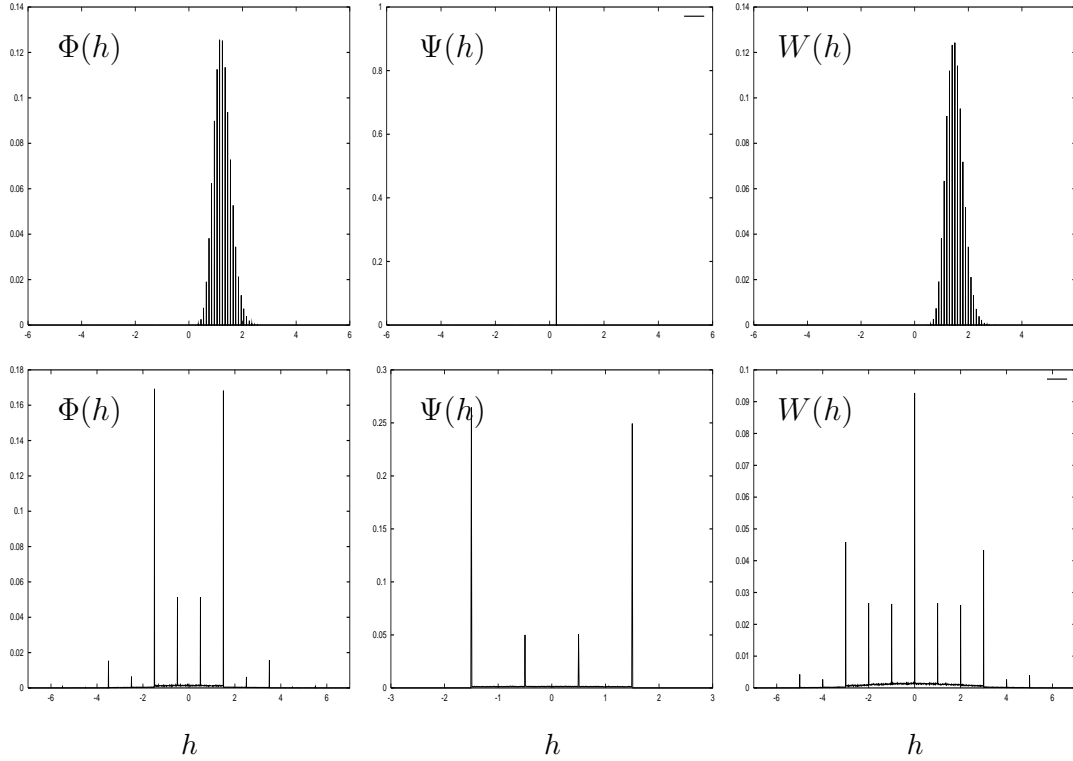
Figure 11. Effective field distributions at zero temperature, for 'small world' magnets (i.e. ferromagnetic rings with random sparse long-range ferromagnetic bonds, top row) and for 'small world' spin glasses (i.e. ferromagnetic rings with random sparse long-range $\pm J$ random bonds). Parameters for the small world magnet are $c = 10$, $J_0 = \frac{1}{4}$, and $J = 1$; for the small world spin-glass they are $c = \frac{1}{2}$, $J_0 = \frac{3}{2}$, $J = 1$ and $p = \frac{5}{8}$. These data strongly suggest that, whereas the small world magnet exhibits zero temperature effective field distributions containing only discrete delta-peaks, those found for small world spin-glasses have additional continuous pieces. This, in turn, might be regarded as evidence for the need to break replica symmetry [33].

replicated transfer matrices, which should have broader applicability). We have applied our theoretical results to two specific cases: the 'small world' ferromagnet (sparse long-range bonds of uniform value) and the 'small world' spin-glass (sparse random $\pm J$ long-range bonds). For these two specific models we could draw explicit RS phase diagrams, and also demonstrate analytically the nontrivial so-called 'small world' effect: for any non-zero value of the bond strength J_0 along the chain (however weak), and any non-zero average Poissonian connectivity c (even $c < 1$) there is always a *finite* temperature phase transition to an ordered state. We have carried out (a limited number of) simulation experiments, which are found to be in good agreement with our theory.

As always, many interesting questions remain to be answered and extensions to be carried out. Firstly, it would be important to find out whether and how replica symmetry needs to be broken in the present model. On the one hand, the fact that the SG transition line in our model is not dependent on p (the probability for a long-range bond to be $+J$) might be seen as a reason to doubt the need for RSB, since it suggests

that in the present models frustration does not play a major role (since for $p = 1$ we would have all ferromagnetic long-range bonds, whereas for $p = -1$ they would be all anti-ferromagnetic). On the other hand, numerical evaluation of the various effective field distributions in our model at $T = 0$ (see figure 11) reveals continuous contributions in the small world spin-glass, which one might take as evidence for RSB. Secondly, one might wonder about and investigate the extent and role of domain formation along the spin chain. Obvious generalizations of our present study would be to other types of long range bond disorder (e.g. Gaussian), other types of spin variables, non-Poissonian random graphs (adapting e.g. the methods of [20]), to anti-ferromagnetic or disordered bonds along the one-dimensional chain (where on the basis of [24] one should expect to find first order transitions), and to include an analysis of correlation and response functions. In one-dimensional systems correlation functions are linked to the second-largest eigenvalue of the transfer matrix. Here we would therefore require further eigenvalues of the replicated transfer matrix; this calculation can be carried out using the formalism of [26], and will be the subject of a future study.

Acknowledgment

References

[1] Watts D J and Strogarz S H 1998 *Nature* **393** 440
[2] Monasson R 1999 *Eur. Phys. J. B.* **12** 555
[3] Barrat A and Weigt M 2000 *Eur. Phys. J.* B **13** 547
[4] Gitterman A 2000 *J. Phys. A: Math. Gen* **33** 8373
[5] Kim B J, Holme P, Jeon G S, Minnagen P and Choi M Y 2001 *Phys. Rev. E* **64** 056135
[6] Herrero C P 2002 *Phys. Rev. E* **65** 066 110
[7] Murayama T, Kabashima Y, Saad D and Vicente R 2000 *Phys. Rev. E* **62** 1577
[8] Nakamura K, Kabashima Y and Saad D 2001 *Europhys. Lett.* **56** 610
[9] Nishimori H 2001 *Statistical Physics of Spin Glasses and Information Processing* (Oxford: University Press)
[10] Kirkpatrick S and Selman B 1994 *Science* **264** 1297
[11] Monasson R and Zecchina R 1998 *Phys. Rev. E* **57** 1357
[12] Monasson R and Zecchina R 1998 *J. Phys. A* **31** 9209
[13] Monasson R, Zecchina R, Kirpatrick S, Selman B and Troyansky L 1999 *Nature* **400** 133
[14] Wemmenhove B and Coolen A C C 2003 *J. Phys. A* **36** 9617
[15] Perez Castillo I and Skantzos N S 2003 *preprint* cond-mat/0309655
[16] Viana L and Bray A J 1985 *J. Phys. C* **18** 3037
[17] Kanter I and Sompolinsky H 1987 *Phys. Rev. Lett.* **58** 164
[18] Mezard M and Parisi G 1987 *Europhys. Lett.* **3** 1067
[19] Mottishaw P and De Dominicis C 1987 *J. Phys. A* **20** L375
[20] Wong K Y and Sherrington D 1988 *J. Phys. A* **21** L459
[21] Monasson R 1998 *J. Phys. A* **31** 513
[22] Mezard A and Parisi G 2001 *Eur. Phys. J. B* **20** 217
[23] Parisi G and Tria F 2002 *preprint* cond-mat/0207144
[24] Skantzos N S and Coolen A C C 2000 *J. Phys. A: Math. Gen* **33** 5785
[25] Sherrington D and Kirkpatrick S 1975 *Phys. Rev. Lett.* **35** 1792
[26] Nikoletopoulos T and Coolen A C C 2004 *in preparation*
[27] Viana Lopes J, Pogorelov Y G, Lopes dos Santos J M B and Toral R 2004 *preprint* cond-mat/0402138
[28] Parisi G 1979 *Phys. Lett.* **73A** 203
[29] Watkin T L H and Sherrington D 1991 *J. Phys. A: Math. Gen.* **24** 5427
[30] Brandt U and Gross W 1978 *Z. Phys. B* **31** 237
[31] Bruinsma R and Aeppli G 1983 *Phys. Rev. Lett.* **50** 1494
[32] Derrida B, Vannimenus J and Pomeau Y 1978 *J. Phys. C* **11** 4749
[33] Mézard M and Parisi G 2003 *J. Stat. Phys.* **111** 1